

*Supporting Information for*

**An Ultrasensitive Lipid Droplet-Targeted NIR Emission Fluorescent Probe for  
Polarity Detection and Its Application in Liver Disease Diagnosis**

Yonghe Tang, Sirui Song, Juanjuan Peng, Qian Zhang, Weiying Lin\*

*Guangxi Key Laboratory of Electrochemical Energy Materials, Institute of Optical Materials and  
Chemical Biology, School of Chemistry and Chemical Engineering, Guangxi University, MOE  
Key Laboratory of New Processing Technology for Nonferrous Metals and Materials, Guangxi  
Key Laboratory of Processing for Non-ferrous Metals and Featured Materials, Nanning, Guangxi  
530004, P. R. China.*

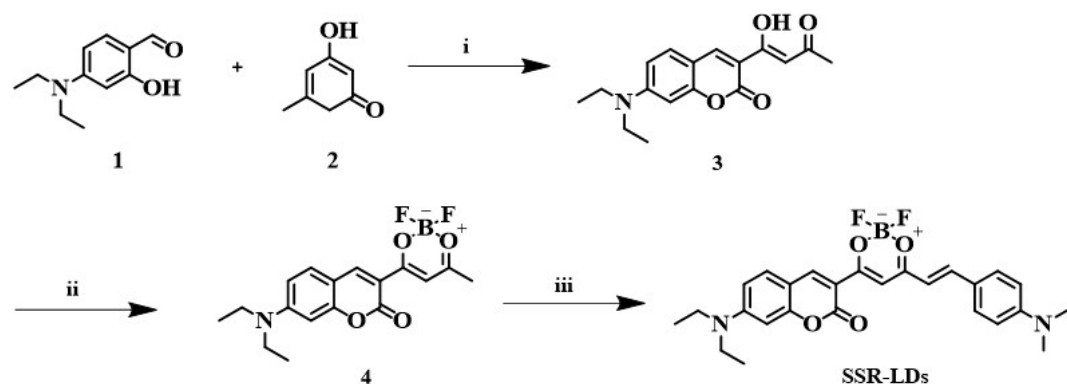
\*Corresponding Author.

*E-mail address:* weiyinglin2013@163.com.

## Table of Contents

Scheme S1.....	S4
Fig. S1.....	S5
Fig. S2.....	S5
Fig. S3.....	S6
Fig. S4.....	S6
Fig. S5.....	S7
Fig. S6.....	S8
Fig. S9.....	S11
Fig. S10.....	S12
Fig. S11.....	S13
Fig. S14.....	S16
Fig. S15.....	S16
Fig. S16.....	S17
Fig. S17.....	S17
Fig. S18.....	S18
Fig. S19.....	S18

**Scheme S1.** Synthesis process of probe SSR-LDs.



Reagents and conditions: (i) Absolute ethanol, 85 °C, 4 h; (ii) anhydrous dichloride, 0 °C, under the protection of nitrogen, 8 h; (iii) 4-(dimethylamino)-benzaldehyde, toluene, room temperature, 24 h.

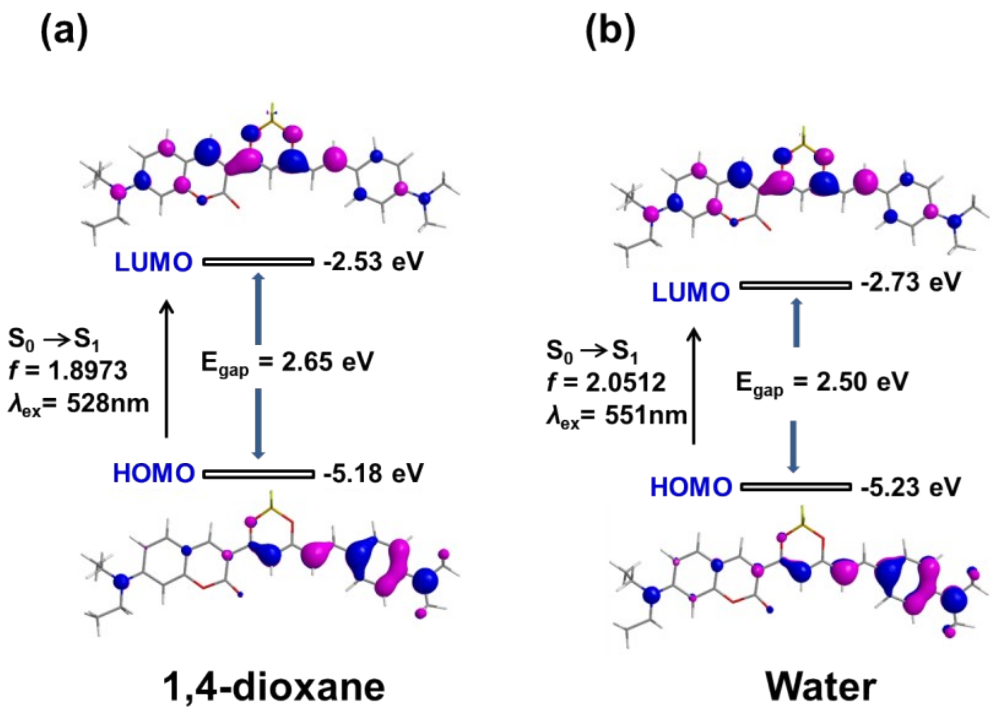


**Fig. S1.** Calculated orbital energy levels and electron density contours of HOMOs and LUMOs for S<sub>0</sub>-optimized geometry and S<sub>1</sub>-optimized geometry of **SSR-LDs** in 1,4-dioxane (a) and water (b), respectively. Transition properties (the energy gap E<sub>gap</sub>, wavelength  $\lambda$ , and oscillator strength  $f$ ) for absorption and emission were also given.

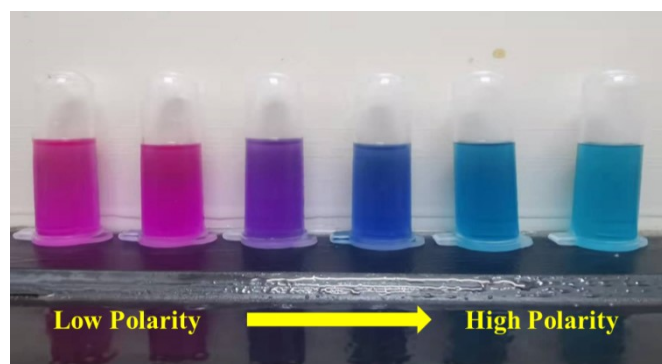


**Fig. S2.** The visual change of solution color of SSR-LDs in different solvents (10 μM). The solvents in sequence: toluene, 1,4-dioxane, tetrahydrofuran (THF), ethanol (ETOH), N,N-dimethylformamide (DMF), dimethyl sulfoxide (DMSO).

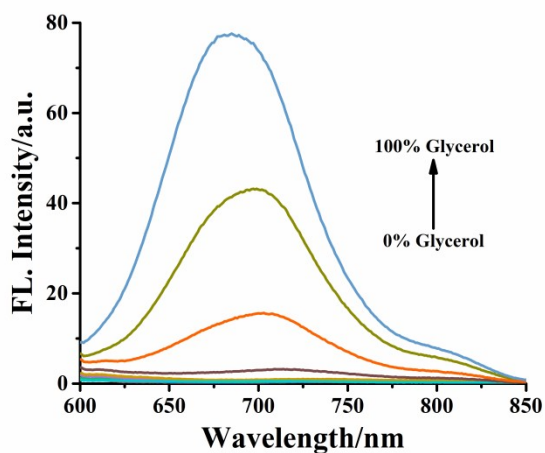


**Fig. S3.** Fluorescence emission spectra of **SSR-LDs** (10  $\mu\text{M}$ ) in different ratios of mixed solvents of PBS and Glycerol.

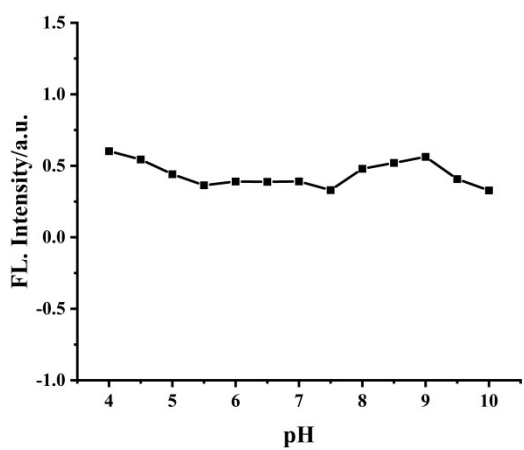


**Fig. S4.** The pH adaptability tests of **SSR-LDs** (10  $\mu\text{M}$ ) at  $\lambda_{\text{ex}}=580$  nm

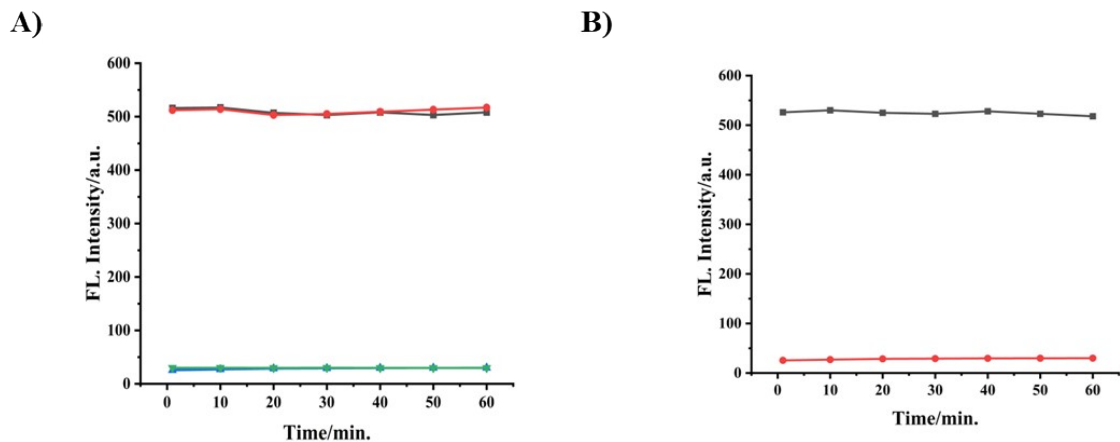


**Fig. S5.** The photo-stability performance test curves of the probe **SSR-LDs** ( $10 \mu\text{M}$ ) in two different polarities solutions (the PBS buffer (red and black), and the mixed solution (1,4-dioxane: PBS = 9:1, v: v) (blue and green)) with different wavelengths (580 nm and 365 nm) of light radiation. A) The photo-stability tests of **SSR-LDs** in the PBS buffer ( $10 \text{ mM}$ , pH 7.4) and the mixed solution (1,4-dioxane: PBS = 9:1, v: v) under light irradiation of 580 nm. B) The photo-stability tests of **SSR-LDs** in the PBS buffer ( $10 \text{ mM}$ , pH 7.4) (red) and the mixed solution (1,4-dioxane: PBS = 9:1, v: v) (black) under light irradiation of 365 nm.

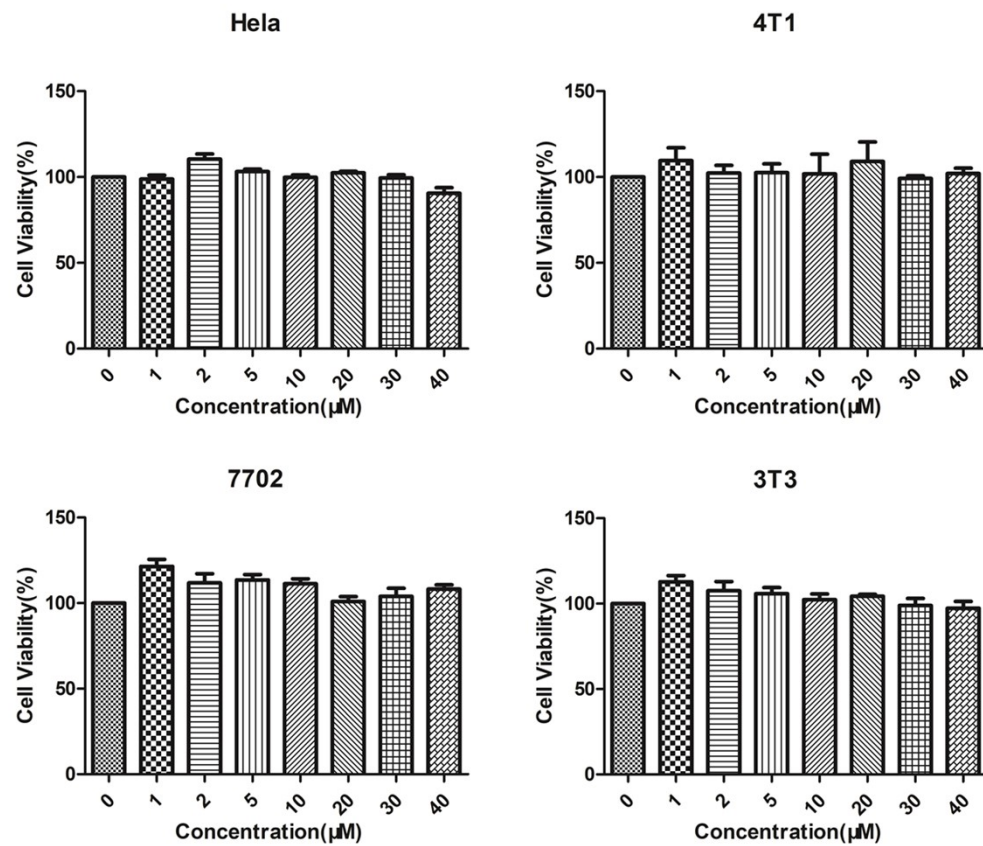


**Fig. S6.** Cytotoxicity tests of four kinds of cell lines (HeLa cells, HL7702 cells, 4T1 cells, and 3T3 cells).

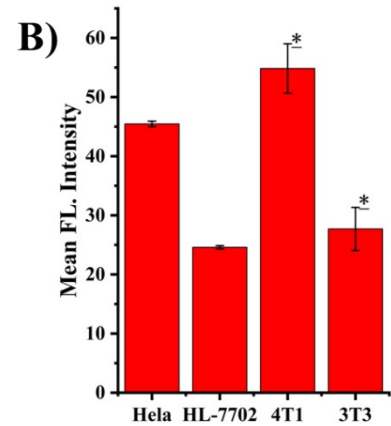
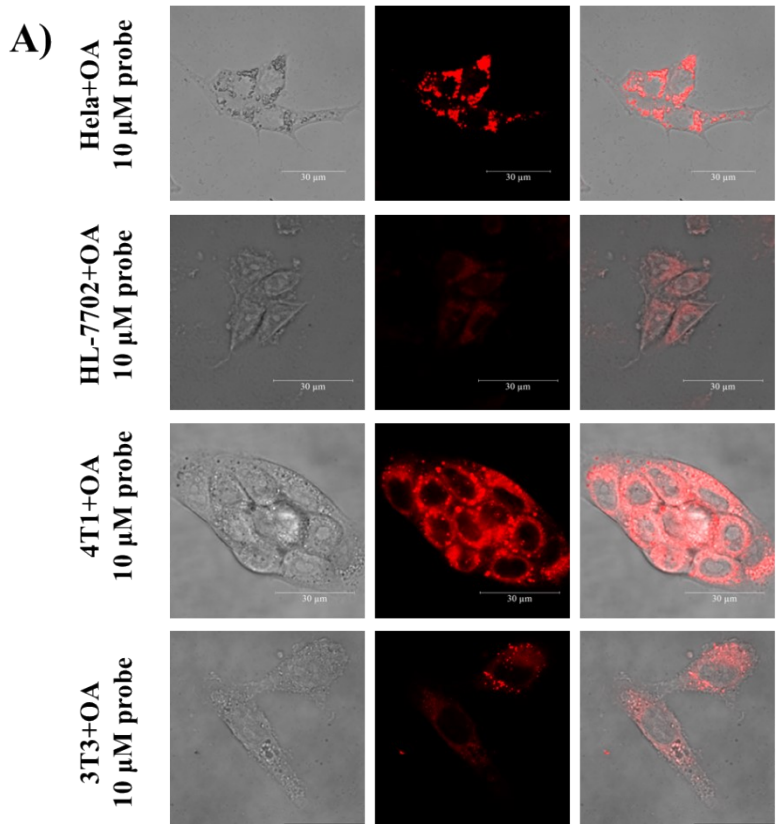


**Fig. S7.** A) Confocal imaging of four different cell lines treated with SSR-LDs (10  $\mu$ M) and OA (400  $\mu$ M). ( $\lambda_{\text{ex}} = 580$ ,  $\lambda_{\text{em}} = 610-750$ ), Scale bar = 30  $\mu$ m; B) The relative fluorescence intensities of the red channels of A). (\*p<0.05).

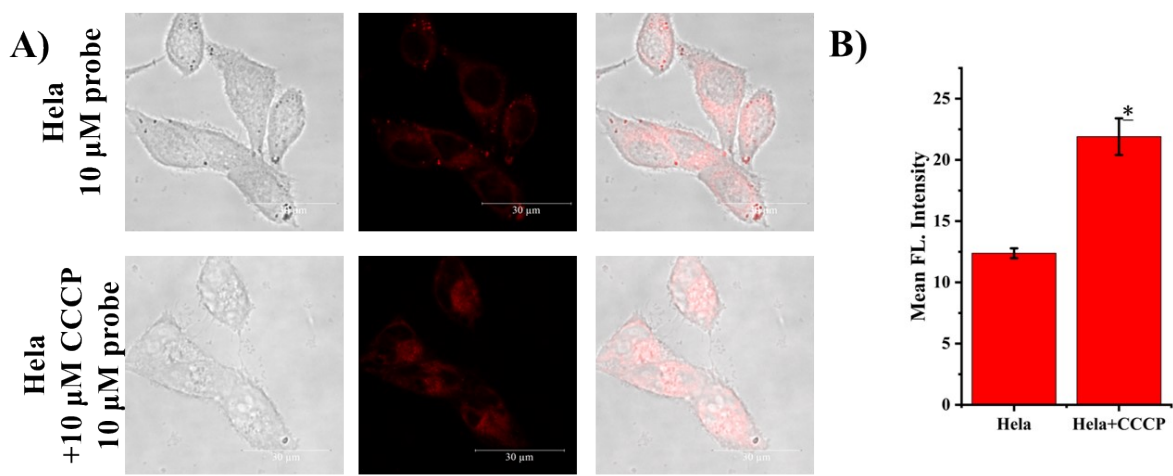


**Fig. S8.** A) The confocal fluorescence imaging of probe **SSR-LDs** (10  $\mu$ M) in living HeLa cells stimulated by CCCP ( $\lambda_{\text{ex}} = 580$ ,  $\lambda_{\text{em}} = 610\text{-}750$ ), Scale bar = 30  $\mu$ m; B) The relative fluorescence intensities of the red channels of A) (\* $p < 0.05$ ).

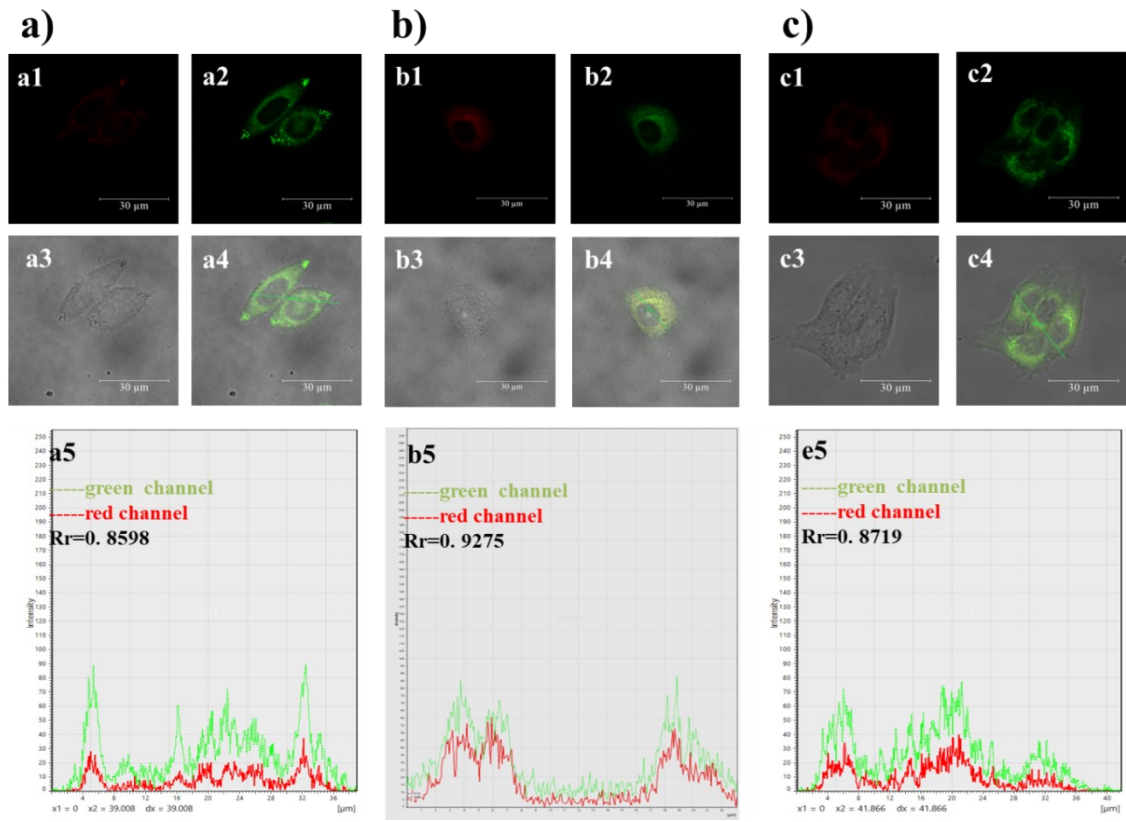


**Fig. S9.** Co-localization imaging of **SSR-LDs** (10  $\mu$ M) and bodipy (200 nM) for imaging three cell lines (HeLa cells, 3T3 cells, and 4T1 cells) pre-treated, Scale bar: 30  $\mu$ M. A) The co-localization imaging of HeLa cells treated with **SSR-LDs** (10  $\mu$ M) and bodipy (200 nM); B) The co-localization imaging of 3T3 cells treated with **SSR-LDs** (10  $\mu$ M) and bodipy (200 nM); C) The co-localization imaging of 4T1 cells treated with **SSR-LDs** (10  $\mu$ M) and bodipy (200 nM). 1) The red channel of **SSR-LDs**; 2) the green channel of bodipy; 3) the bright field channel; 4) the merge of 1-3); 5) Intensity profile of **SSR-LDs** in the red channel and bodipy in green channel. Green channel:  $\lambda_{ex}$ : 580 nm, collected 610 nm-750 nm.

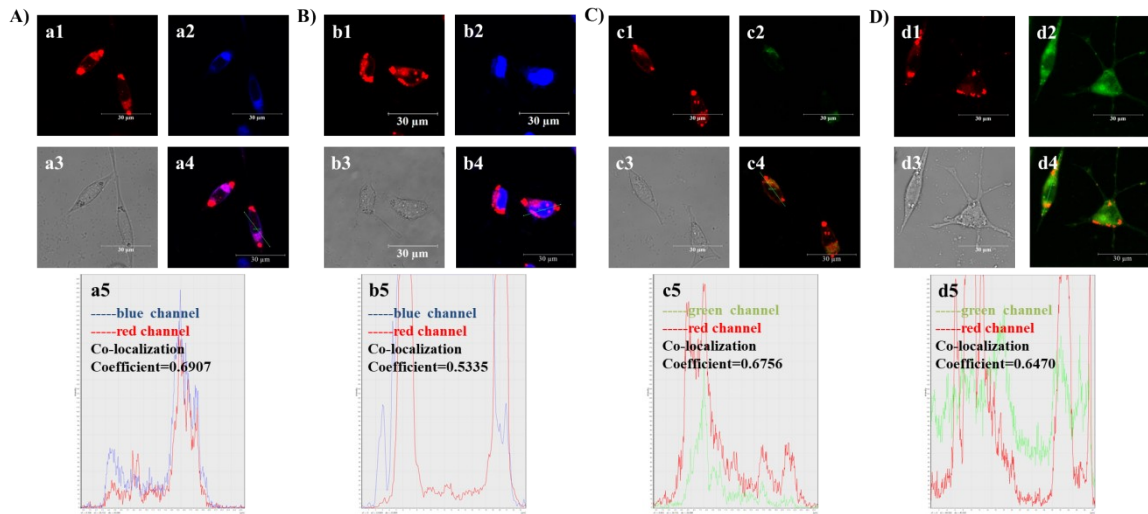


**Fig. S10.** Co-localization imaging of **SSR-LDs** (10  $\mu$ M) and different organelle localization dyes in HeLa cells, Scale bar: 30  $\mu$ M. A) The co-localization imaging of HeLa cells treated with **SSR-LDs** (10  $\mu$ M) and ER tracker blue (200 nM). B) The co-localization imaging of HeLa cells treated with **SSR-LDs** (10  $\mu$ M) and Hoechst 33342 (200 nM). C) The co-localization imaging of HeLa cells treated with **SSR-LDs** (10  $\mu$ M) and Lyso Tracker green (200 nM). D) The co-localization imaging of HeLa cells treated with **SSR-LDs** (10  $\mu$ M) and Mito Tracker green (200 nM).

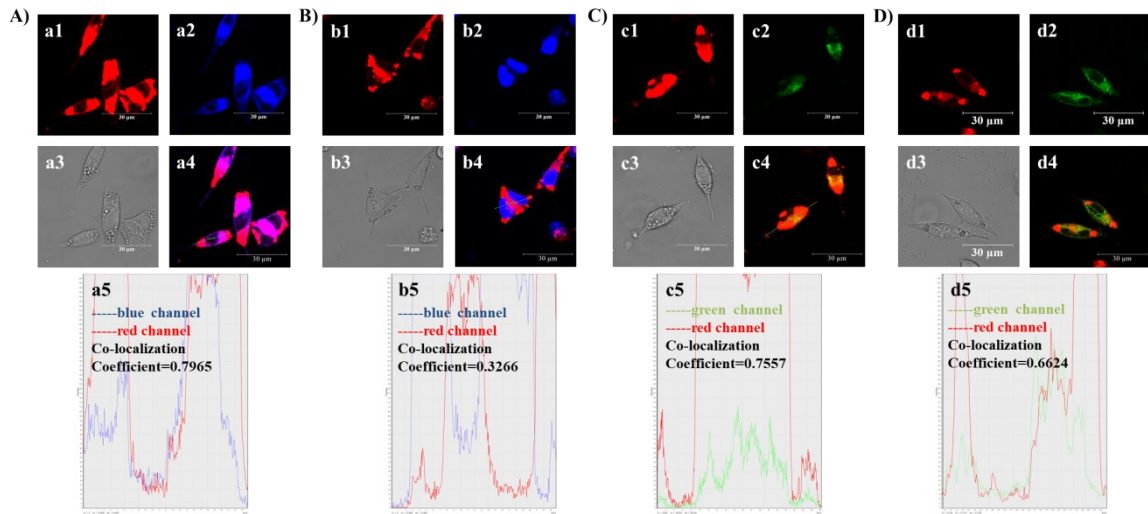


**Fig. S11.** Co-localization imaging of **SSR-LDs** (10  $\mu\text{M}$ ) and different organelle localization dyes in HeLa cells pre-treated with OA (400  $\mu\text{M}$ ). Scale bar: 30  $\mu\text{M}$ . A) The co-localization imaging of HeLa cells pre-treated with OA (400  $\mu\text{M}$ ), then treated with **SSR-LDs** (10  $\mu\text{M}$ ) and ER tracker blue (200 nM). B) The co-localization imaging of HeLa cells pre-treated with OA (400  $\mu\text{M}$ ), then treated with **SSR-LDs** (10  $\mu\text{M}$ ) and Hoechst 33342 (200 nM). C) The co-localization imaging of HeLa cells pre-treated with OA (400  $\mu\text{M}$ ), then treated with **SSR-LDs** (10  $\mu\text{M}$ ) and Lyso Tracker green (200 nM). D) The co-localization imaging of HeLa cells pre-treated with OA (400  $\mu\text{M}$ ), then treated with **SSR-LDs** (10  $\mu\text{M}$ ) and Mito Tracker green (200 nM).

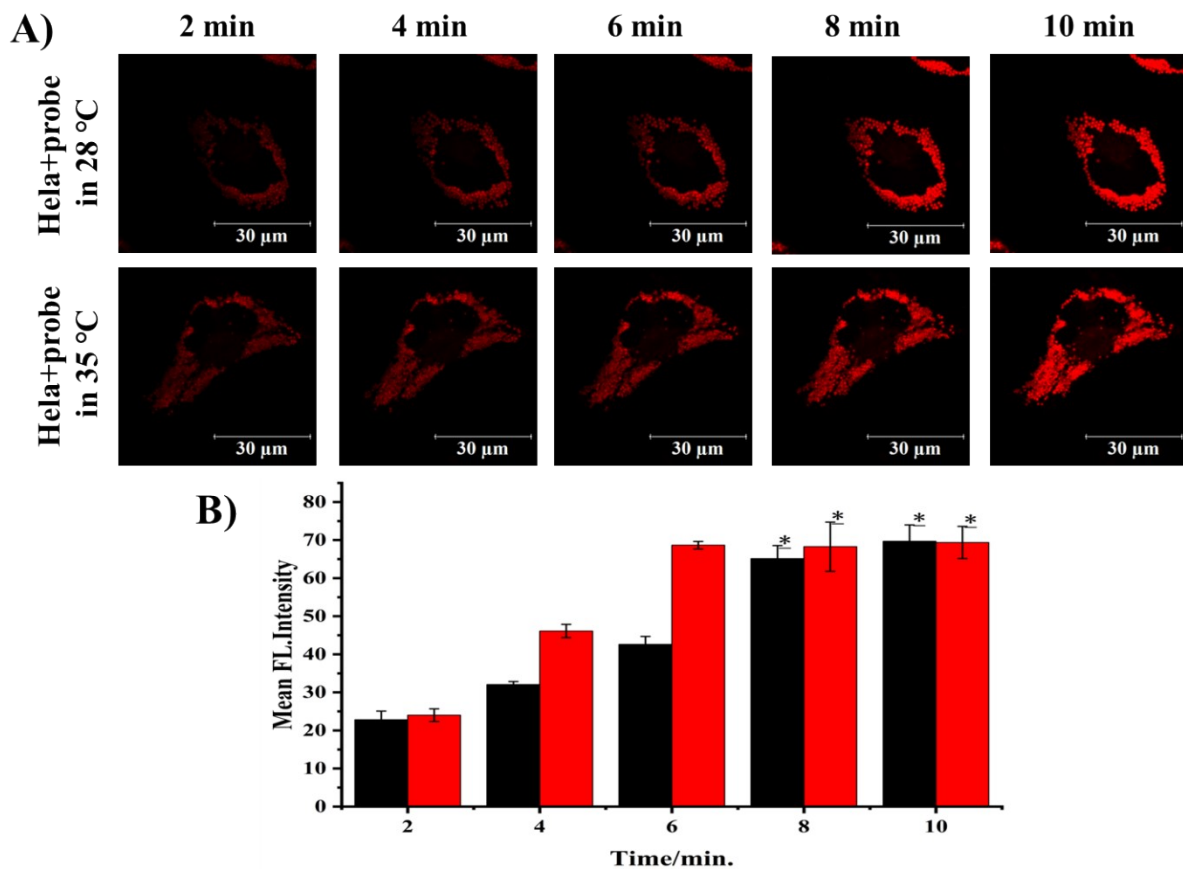


**Fig. S12.** A) Time-dependent confocal fluorescence imaging of the probe SSR-LDs (10  $\mu\text{M}$ ) at different temperatures in living Hela cells treated with OA (28 °C and 35 °C) ( $\lambda_{\text{ex}} = 580$ ,  $\lambda_{\text{em}} = 610\text{-}750$ ), Scale bar = 30  $\mu\text{m}$ . B) The relative fluorescence intensities of the red channels of A). (black represents 28 °C and red represents 35 °C) (\*p<0.05).

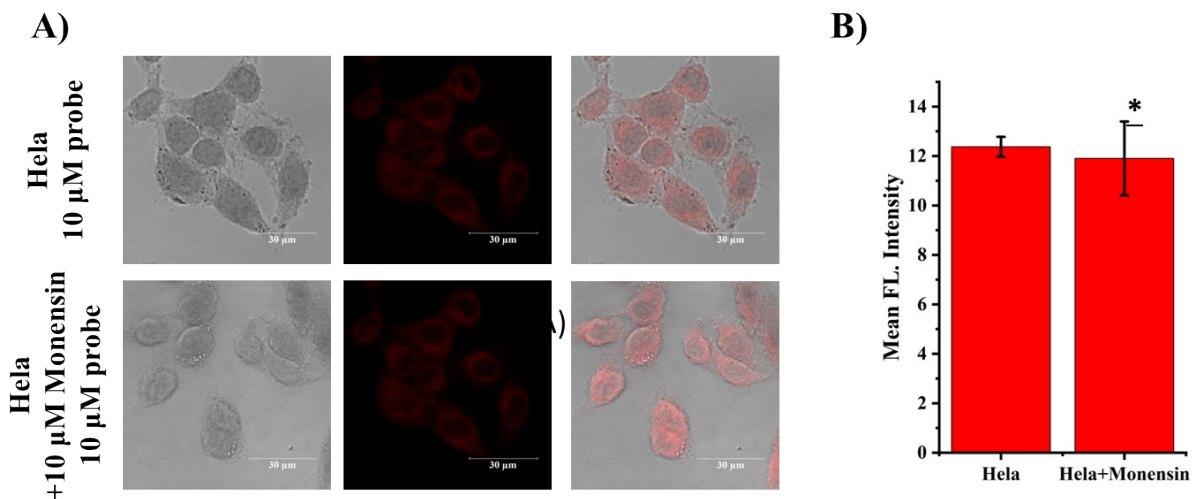


**Fig. S13.** A) The confocal fluorescence imaging of probe **SSR-LDs** (10  $\mu$ M) in living HeLa cells stimulated by monensin ( $\lambda_{\text{ex}} = 580$ ,  $\lambda_{\text{em}} = 610\text{-}750$ ), Scale bar = 30  $\mu$ m; B) The relative fluorescence intensities of the red channels of A) (\* $p < 0.05$ ).

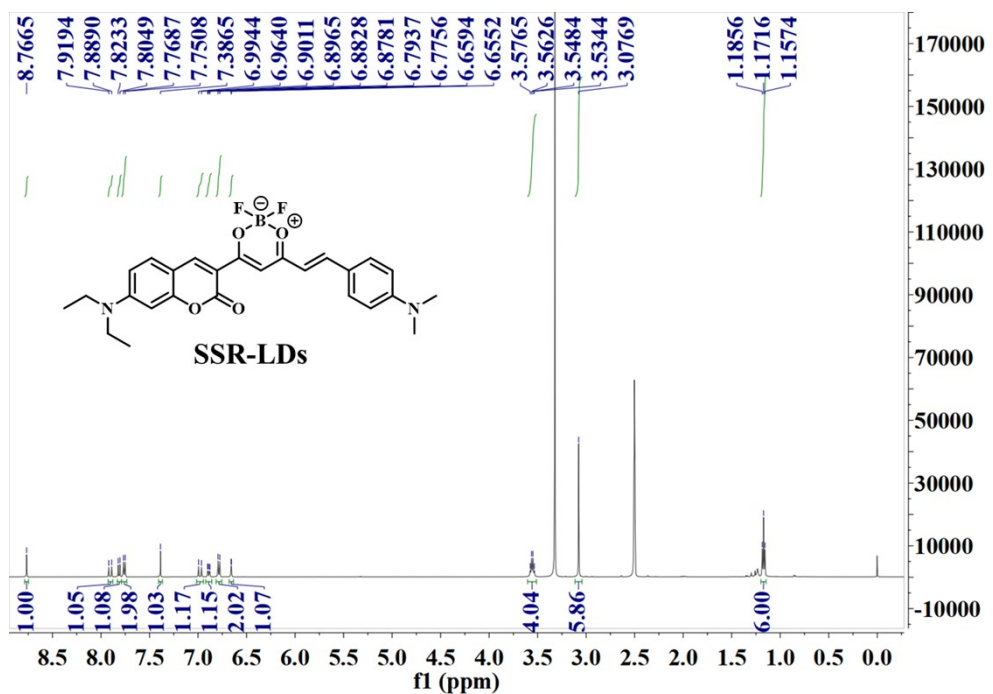


**Fig. S14.** <sup>1</sup>H NMR (DMSO-*d*<sub>6</sub>) spectrum of SSR-LDs.

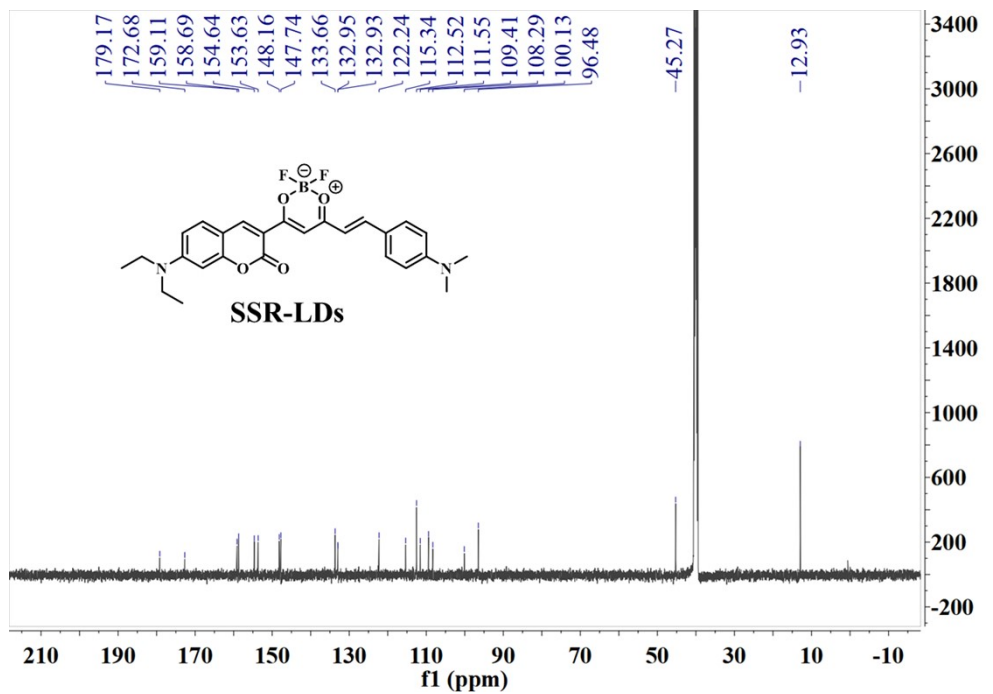


**Fig. S15.** <sup>13</sup>C NMR (DMSO-*d*<sub>6</sub>) spectrum of SSR-LDs.

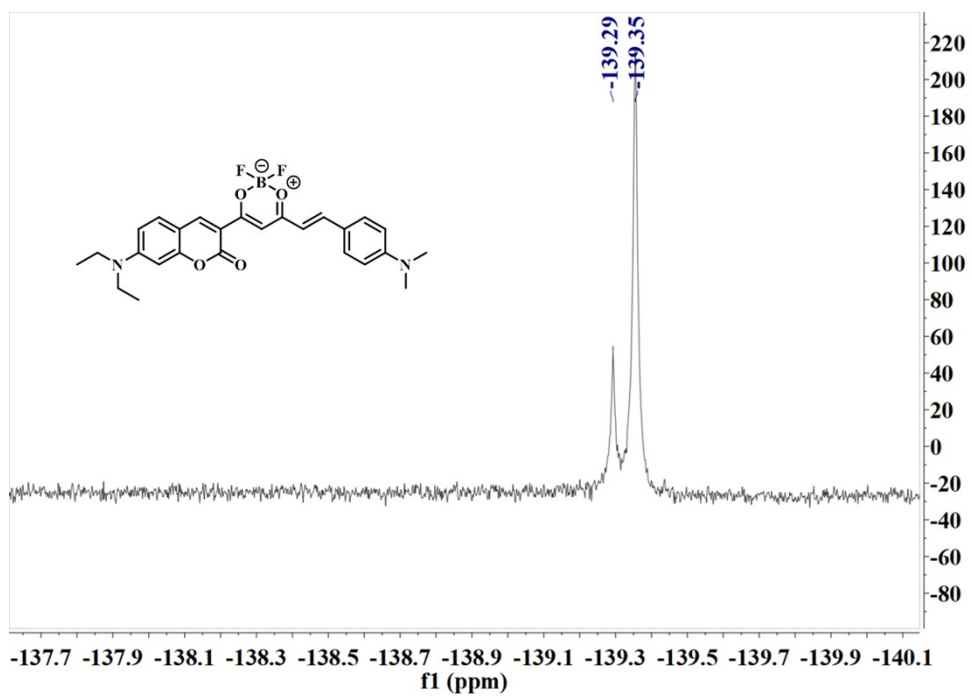


**Fig. S16.**  $^{19}\text{F}$  NMR ( $\text{DMSO}-d_6$ ) spectrum of SSR-LDs.

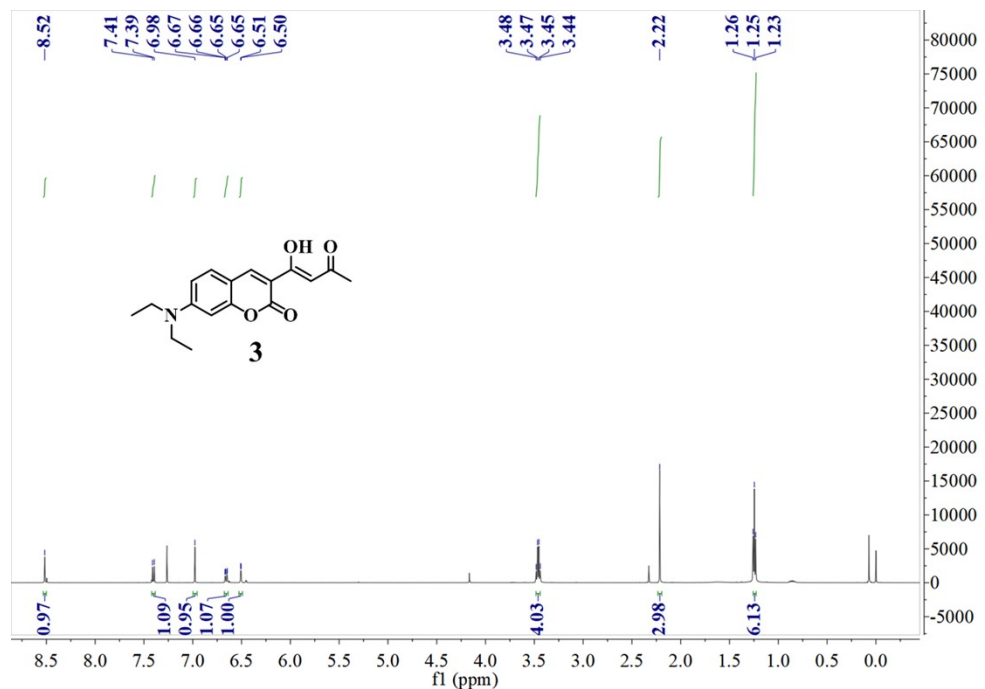


**Fig. S17.**  $^1\text{H}$  NMR ( $\text{CDCl}_3-d$ ) spectrum of compound 3.

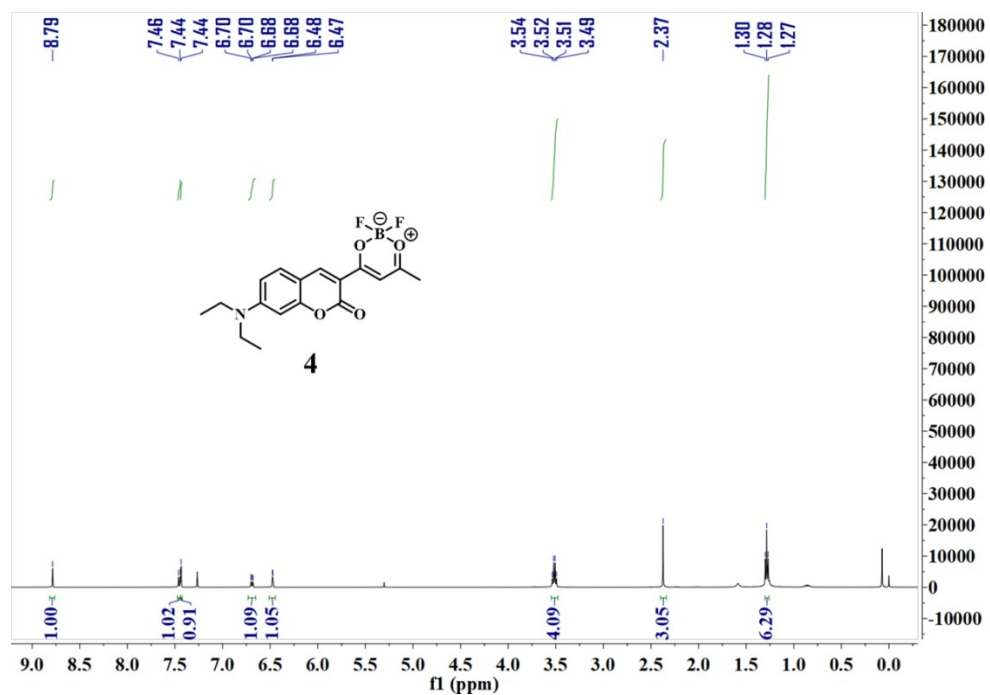


**Fig. S18.**  $^1\text{H}$  NMR ( $\text{CDCl}_3\text{-}d$ ) spectrum of compound 4.

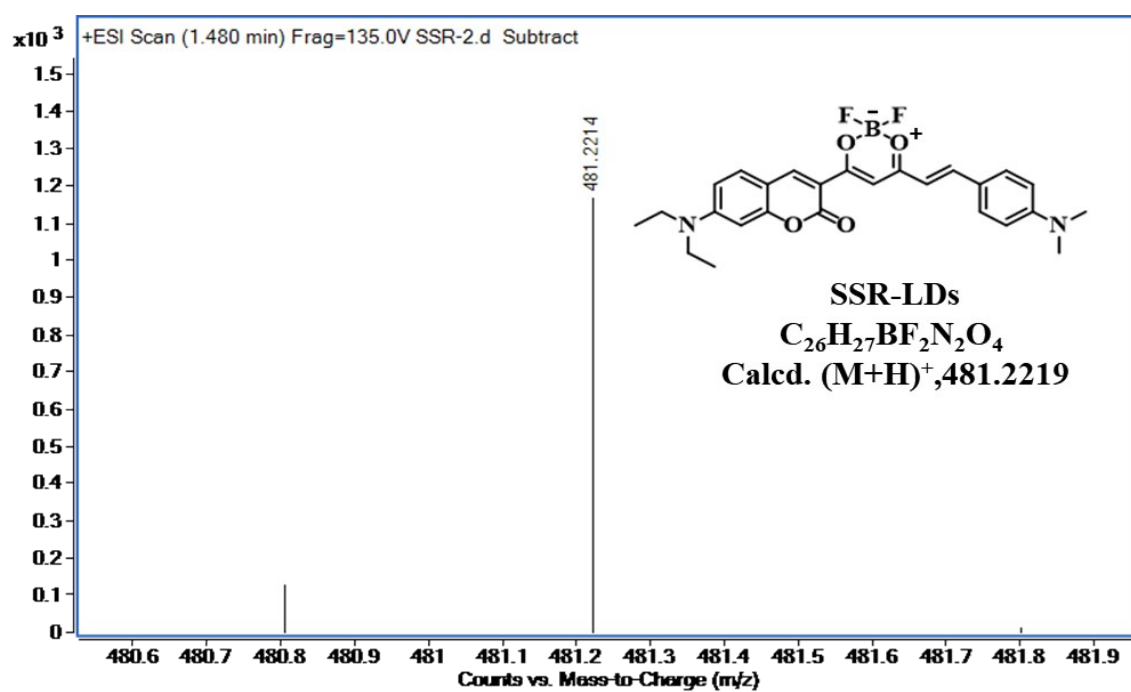


**Fig. S19.** HR-MS (ESI) spectrum of SSR-LDs,  $(\text{M}+\text{H})^+$ , 481.2219.